

Efficient Computation of Aerodynamic Noise

Georgi S. Djambazov, Choi-Hong Lai, and Koulis A. Pericleous

1. Introduction

Computational Fluid Dynamics codes based on the Reynolds averaged Navier-Stokes equations may be used to simulate the generation of sound waves along with the other features of the flow of air. For adequate acoustic modeling the information about the sound sources within the flow is passed to a linearized Euler solver that accurately resolves the propagation of sound through the non-uniformly moving medium.

Aerodynamic sound is generated by the flow of air or results from the interaction of sound with airflow. Computation of aerodynamic noise implies *direct* simulation of the sound field based on first principles [6]. It allows complex sound fields to be simulated such as those arising in turbulent flows.

When building a software tool for this simulation two options exist: (a) to develop a new code especially for this purpose, or (b) to use an existing Computational Fluid Dynamics (CFD) code as much as possible. (As it will be shown later, due to numerical diffusion conventional CFD codes tend to smear the sound signal too close to its source, and cannot be used directly for aeroacoustic simulations.)

The second option is considered here as it seems to require less work and makes use of the vast amount of experience accumulated in flow modeling. CFD codes have built-in capabilities of handling non-linearities, curved boundaries, boundary layers, turbulence, and thermal effects. They are based on optimized, efficient, readily converging algorithms. If no CFD code is used as a basis, all these features have to be implemented again in the new code developed for the simulation of the sound field.

2. The need for a special approach to sound

Aerodynamic sound is generated as a result of the interaction of vortex structures that arise in viscous flows. These vortex structures are most often associated with either a shear layer or a solid surface. Once the sound is generated it propagates in the surrounding non-uniformly moving medium and travels to the ‘far field’.

Sound propagation is hardly affected by viscosity (that is why noise is so difficult to suppress). Also, sound perturbations are so small that their contribution to the

1991 *Mathematics Subject Classification*. Primary 65M60; Secondary 76D05.

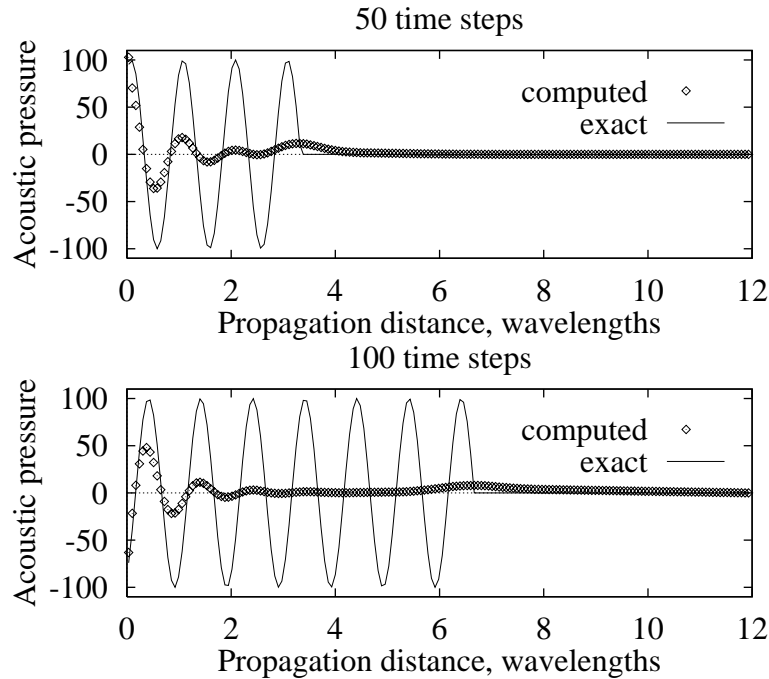


FIGURE 1. Conventional CFD solution of test problem

convection velocity of the flow is negligible in many cases. These two facts mean that sound propagation is, in essence, described by the linearized Euler equations (1).

The simulation of the flow that generates sound, however, requires time accurate solutions of the Navier-Stokes equations. Two approaches exist here: Reynolds Averages and Large Eddy Simulation. Both of them require adequate turbulence models and fine meshes to capture the small structures in the flow that oscillate and generate sound.

Most available Computational Fluid Dynamics (CFD) codes have implementations of Reynolds Averaged Navier-Stokes solvers (RANS). That is because the new alternative, Large Eddy Simulation (LES), requires more computational power that has become available only in the recent years. In our opinion, the future of Computational Aeroacoustics (CAA) is closely related to LES. For the time being, however, we should try to make the most of RANS.

Due to the diffusivity of the numerical schemes and the extremely small magnitude of the sound perturbations, RANS codes are not generally configured to simulate sound wave propagation. This is illustrated by the simple test of one-dimensional propagation in a tube of sound waves generated by a piston at one end that starts oscillating at time zero. The resulting sound field (pressure distribution) is compared with the one computed by the RANS solver PHOENICS [1] with its default numerical scheme (upwind fully implicit). As it can be seen on Figure 1, the numerical and the analytic solutions agree only in a very narrow region next to the source at the left end of the domain. In this admittedly worst-case scenario,

TABLE 1

<u>CFD</u>	<u>CAA</u>
(Computational Fluid Dynamics)	(Computational Aeroacoustics)
Nonuniform/Unstructured Grid	Regular Cartesian Grid
Fully Implicit in Time	Explicit/semi-implicit Schemes
Upwind Discretization	Higher Order Numerical Schemes
Smooth Solid Boundaries	Boundaries Can Be Stepwise
Small-scale structures	Extremely small magnitude

refining of the mesh does not change the result at all. (Better results can be obtained by switching to higher order schemes available within the same CFD code but they still cannot be relied upon for long distance wave propagation.)

To tackle these problems the new scientific discipline Computational Aeroacoustics has emerged in the last several years. The important issues of sound simulation have been identified [7], and adequate methods have been developed [8, 4, 3]. Table 1 shows how different the requirements for *accuracy* and *efficiency* are with the numerical solutions of the flow and the sound field respectively.

Although the sound equations (1) are a particular form of the equations governing fluid flow, great differences exist in magnitude, energy and scale of the solved-for quantities. (Acoustic perturbations are typically at least 10 times weaker than the corresponding hydrodynamic perturbations and a thousand times smaller than the mean flow that carries them. On the other hand acoustic wavelengths are typically several times larger than the corresponding structures in the flow.)

All this means that the algorithmic implementations are so different that they can hardly share any software modules. So, it will be best if a way is found of coupling a flow solver with an acoustic solver in such a manner that each of them does the job that it is best suited for.

3. The coupling

The basic idea of software coupling between CFD and CAA (decomposition of variables into flow and acoustic parts) as well as the Domain Decomposition into near field and far field was presented in our previous works [2, 3]. The CFD code is used to solve the time-dependent RANS equations while the CAA deals with the linearized Euler equations:

$$(1) \quad \begin{aligned} \frac{\partial p}{\partial t} + \bar{v}_j \frac{\partial p}{\partial x_j} + \bar{\rho} c^2 \frac{\partial v_j}{\partial x_j} &= S \\ \frac{\partial v_i}{\partial t} + \bar{v}_j \frac{\partial v_i}{\partial x_j} + \frac{1}{\bar{\rho}} \frac{\partial p}{\partial x_i} &= F_i. \end{aligned}$$

Here p is the pressure perturbation, v_1, v_2 and v_3 are the Cartesian components of the velocity perturbation. The values of the speed of sound c , of the local density $\bar{\rho}$ and of the velocity components of the flow \bar{v}_j are supplied by the CFD code.

CAA algorithms are designed to solve these equations (1) with known right-hand sides S and F_i that are functions of x_i and time t . Term S contains any sources of mass that may be present in the computational domain, such as vibrating solid surfaces. The three forcing terms F_i will be set to zero in most practical acoustic applications. In theory they contain the viscous forces which have negligible effect on sound propagation. There are some cases where the nonlinear terms associated with the acoustic perturbations may have to be taken into account. Then S and F_i will be updated within the acoustic code at each iteration rather than once per time step.

The present study concentrates on the use of the source term S to transfer the information about the generation of sound from the CFD code to the acoustic solver.

A closer examination of the time history of the CFD solution pictured in Figure 1 reveals that the pressure at the first node next to the source of sound has been resolved accurately. It is suggested that the temporal derivative of the local pressure at the source nodes, calculated from the CFD solution, is added to the source term S of the acoustic equations (1).

$$(2) \quad S = \frac{\partial \bar{p}}{\partial t} + S_{vib}$$

Here S_{vib} denotes sources external to the flow like vibrating solid objects. Thus the following combined algorithm can be outlined:

1. Obtain a steady CFD solution of the flow problem.
2. Start the time-dependent CFD simulation with these initial conditions.
3. Impose the calculated temporal derivative of the pressure at selected nodes within the flow region as part of the source term of the acoustic simulation.
4. Solve the linearized Euler equations in the acoustic domain applying any external sources of mass (vibrating solids).

The introduction of the temporal derivative $\frac{\partial \bar{p}}{\partial t}$ into the source term S is best implemented in finite volume discretization. Then, if phase accuracy of the calculated acoustic signal is essential (like with resonance), the time-dependent outflow from the control volume with increasing \bar{p} in the CFD solution or the inflow perturbation if \bar{p} is decreasing should also be taken into account in order to calculate the correct amount of mass that is assumed to enter or exit the acoustic simulation at each time step. The finite volume form of the RANS continuity equation with isentropic conditions ($\frac{\partial \bar{p}}{\partial p} = c^2$) suggests the following pressure source:

$$(3) \quad \begin{aligned} S &= \bar{\rho} c^2 (\bar{v}_j - \overline{v_{j,average}}) \frac{A_j}{\Delta V} + S_{vib} \\ j &= Influx, \frac{\partial \bar{p}}{\partial t} > 0 \\ j &= Outflow, \frac{\partial \bar{p}}{\partial t} < 0 \end{aligned}$$

where A_{Influx} is the area of the faces of the cell with volume ΔV across which there is inflow during the time step Δt , and the repeated index denotes summation over all such faces. Since this option introduces the whole flow perturbation into

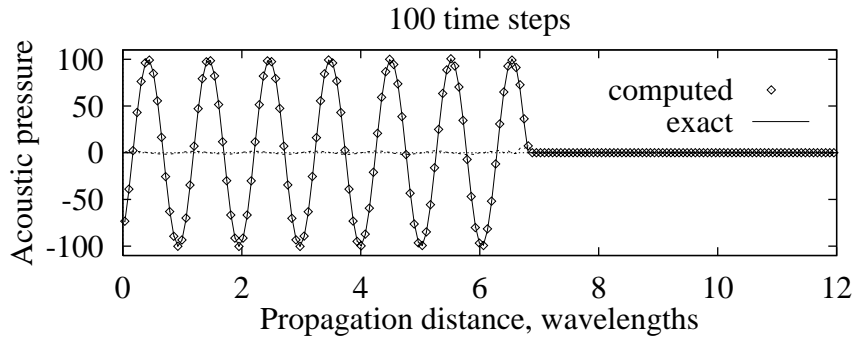


FIGURE 2. Combined solution of test problem

the acoustic simulation, the acoustic solver in this case must be capable of handling smooth curved solid boundaries.

The two codes have separate meshes in overlapping domains. The RANS mesh must be body fitted to represent smooth solid boundaries. The acoustic mesh can be regular Cartesian if option (2) is chosen. In this case the CAA domain can be larger — extending to the mid field if Kirchhoff’s method is used [5] or to the far field if high-order optimized numerical schemes are employed [8]. Uniform mean flow has to be assumed outside the region of the CFD simulation.

Prior to the introduction into the acoustic simulation the flow quantities ($\overline{v_j}, \overline{\rho}$ and \overline{p} , in air $c^2 = 1.4 \frac{\overline{p}}{\overline{\rho}}$, see 1) are interpolated with piecewise constant functions (choosing the nearest neighbouring point from the irregular CFD mesh). This can be done because typically the flow mesh is finer than the acoustic mesh.

In some cases (separated flows, jets) the sources of noise cannot be localized and are instead distributed across the computational domain. Then the most efficient option is choosing a higher order scheme within the CFD code itself and defining a ‘near field’ boundary where the acoustic signal is radiated from the RANS solver to the linearized Euler solver.

4. Results

The above algorithm was validated on the same 1D propagation test problem that was described in the second section. Using the pressure, velocity and density fields provided by the CFD code at each time step and a finite volume acoustic solver, the actual acoustic signal was recovered as it can be seen in Figure 2. Here the coupling option defined by (3) has been implemented with $S_{vib} = 0$. (The acoustic source was introduced in the CFD simulation rather than in the acoustic one, in order to set up this test.)

As a 2D example, generation of sound by a vortex impinging on a flat plate is considered. A Reynolds-Averaged Navier-Stokes solver [1] is used to compute the airflow on a mesh that is two times finer in the direction perpendicular to the plate than the corresponding grid for adequate acoustic simulation.

The geometry of the problem and the hydrodynamic perturbation velocity field (with the uniform background flow subtracted) are in Figure 3.

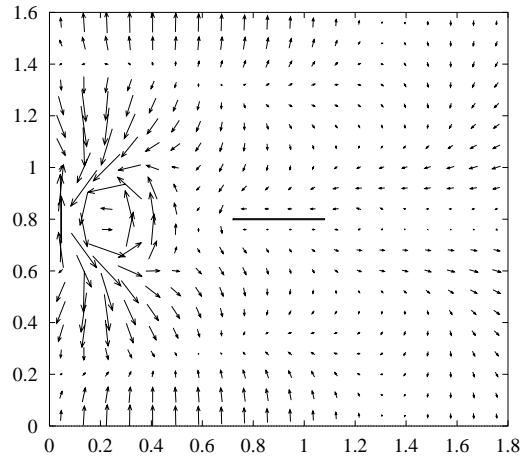


FIGURE 3. Hydrodynamic perturbations and blade. Scale: 1 m/s to 0.1 m

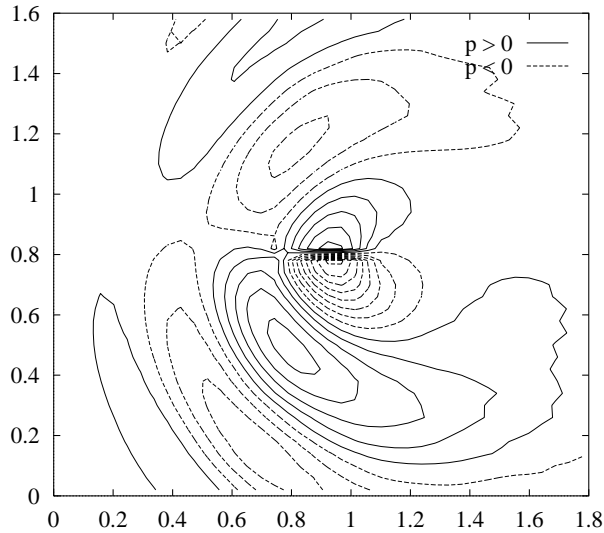


FIGURE 4. Instantaneous pressure contours. Spacing: 6 Pa

The pressure fluctuations (temporal derivatives) next to the solid surface are imposed as source terms on the linearised Euler equations which are solved separately as described above. The size of the computational domain is small enough so that the finite volume solver [3] can predict accurately the sound field. A snapshot of the pressure perturbations can be seen in Figure 4. A graph was made of the acoustic pressure as a function of time at different locations above and below the solid blade. As it can be seen from Figure 5, the amplitude of the sound waves generated at the blade decreases away from it as expected.

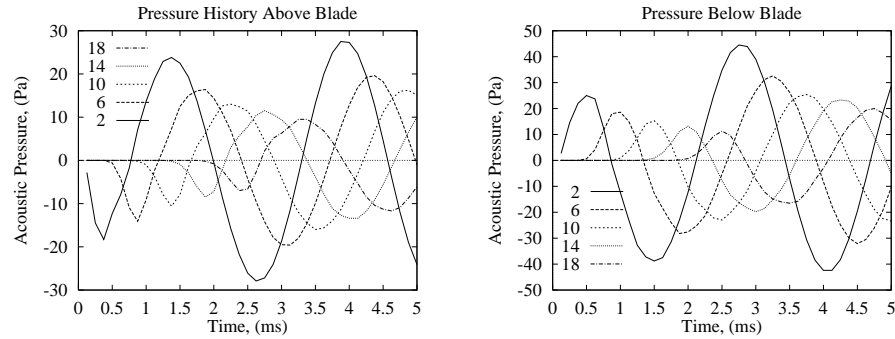


FIGURE 5. Acoustic signal in the specified cells above and below the centre of the blade.

5. Conclusions

A coupled technique has been developed that allows general-purpose RANS solvers to be used with sound generation problems. Both geometrical and physical domain decomposition has been considered. At the locations where it is generated sound is passed to a linearized Euler solver that allows adequate numerical representation of the propagating acoustic waves. The current implementation is applicable to aerodynamic noise generation either on solid surfaces or in volumes that are not surrounded by reflecting objects.

References

1. CHAM Ltd, Wimbledon, UK, *Phoenixics*.
2. G.S. Djambazov, C.-H. Lai, and K.A. Pericleous, *Development of a domain decomposition method for computational aeroacoustics*, DD9 Proceedings, John Wiley & Sons, 1997.
3. ———, *Domain decomposition methods for some aerodynamic noise problems*, 3rd AIAA/CEAS Aeroacoustics Conference, no. 97-1608, 1997, pp. 191–198.
4. ———, *Testing a linear propagation module on some acoustic scattering problems*, Second Computational Aeroacoustics Workshop on Benchmark Problems, Conference Publications, no. 3352, NASA, 1997, pp. 221–229.
5. Anastasios S. Lyrintzis, *The use of Kirchhoff's method in computational aeroacoustics*, ASME-FED **147** (1993), 53–61.
6. A.D. Pierce, *Validation methodology: Review and comments*, Computational Aeroacoustics, Springer-Verlag New York, Inc., 1993, pp. 169–173.
7. C.K.W. Tam, *Computational aeroacoustics: Issues and methods*, AIAA Journal **33** (1995), no. 10, 1788–1796.
8. C.K.W. Tam and J.C. Webb, *Dispersion-relation-preserving finite difference schemes for computational acoustics*, Journal of Computational Physics **107** (1993), 262–281.

SCHOOL OF COMPUTING AND MATHEMATICAL SCIENCES, UNIVERSITY OF GREENWICH, WEL-
LINGTON STREET, WOOLWICH, LONDON SE18 6PF, U.K.

E-mail address: G.Djambazov@gre.ac.uk

SCHOOL OF COMPUTING AND MATHEMATICAL SCIENCES, UNIVERSITY OF GREENWICH, WEL-
LINGTON STREET, WOOLWICH, LONDON SE18 6PF, U.K.

E-mail address: C.H.Lai@gre.ac.uk

SCHOOL OF COMPUTING AND MATHEMATICAL SCIENCES, UNIVERSITY OF GREENWICH, WEL-
LINGTON STREET, WOOLWICH, LONDON SE18 6PF, U.K.

E-mail address: K.Pericleous@gre.ac.uk